J. Fluid Mech. (1979), *vol.* 90, *part* 4, *pp.* 625–639
Printed in Great Britain

Swirling water bells

By FRITZ H. BARK, HANS-PETER WALLIN
Department of Mechanics, Royal Institute of Technology, Stockholm, Sweden
MARCUS G. GÄLLSTEDT
Department of Hydromechanics, Royal Institute of Technology, Stockholm, Sweden
AND L. PETER KRISTIANSSON
Department of Mechanics, Royal Institute of Technology, Stockholm, Sweden

(Received 27 January 1978 and in revised form 15 August 1978)

Swirling water bells are studied theoretically and experimentally. It is shown theoretically that, if the effects of gravity and the surrounding air are neglected, the shape of a swirling water bell will, under certain circumstances, be periodic along the axis of rotation. Under ideal conditions, a swirling water bell may thus be infinitely long. However, the experiments show that in reality the length of a swirling water bell will be limited owing to Kelvin–Helmholtz instabilities. Theoretically calculated shapes of swirling water bells are found to agree reasonably well with experimental results.

1. Introduction

A water bell is an axisymmetric thin sheet of water which moves freely in the surrounding air and has a bell-like shape. The dynamics of water bells are characterized by a balance between inertia and surface tension and are modified by gravity and the induced motion of the surrounding air. Flows of this kind were first investigated experimentally in the very thorough studies by Savart (1833, 1834). The governing equations for the case when the motion of the surrounding air can be neglected, which is a good approximation unless the sheet is very thin and moves very rapidly (Wegener & Parlange 1964; Parlange 1967), were first derived by Boussinesq (1869, 1913). The equations given by Boussinesq were written in dimensionless form by Taylor (1959*a*), who also found an exact solution for the case when the gravitational force can be neglected. Taylor (1959*a*) also made experiments and the theoretical predictions were in good agreement with the experimental results.

In the present work, swirling water bells are investigated theoretically and experimentally. This kind of flow is used in fan spray nozzles (e.g. see Dombrowski, Hasson & Ward 1960). A new application has been suggested by Stenström (1971), who pointed out that placing a milk bell in a microwave field may be a useful way to sterilize milk which eliminates the risk of burning at solid surfaces. In this application one of the key problems is to manipulate the time spent by a liquid particle in the portion of space occupied by the microwave field. Rotation of the bell thus provides a useful extra degree of freedom to control this parameter.

The plan of the paper is as follows. The governing equations for a swirling water

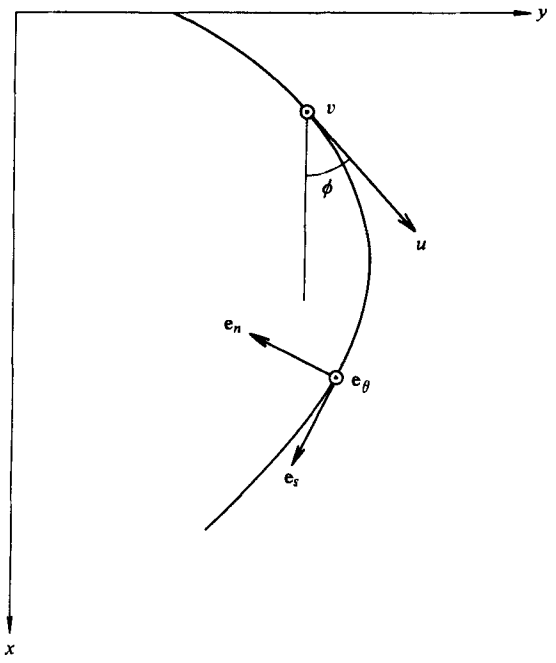

FIGURE 1. Definition of co-ordinate system.

bell are derived in § 2. A perturbation solution of these equations for a slowly rotating water bell is given in § 3. Some general properties of swirling water bells are discussed in § 4. The experimental equipment is briefly described in § 5. In § 6, the experimental results are discussed and some comparisons with theoretical predictions are made.

2. Governing equations

Consider a thin swirling sheet of water which is symmetric about the axis of rotation. A fixed Cartesian co-ordinate system is introduced with the x axis coinciding with the axis of rotation. Figure 1 shows the part of the contour of the water bell in the x, y plane. The bell starts at the point $(0, y_0)$ with a slope given by the angle ϕ_0. In the derivation of the equations for the motion of the water, the following quantities will be used:

h, local thickness of the water sheet;
ρ, density of the water;
g, gravitational acceleration, which is assumed to be in the $\mathbf{e}_x$ direction;
Γ, surface tension;
p, pressure difference between the two sides of the sheet;
λ, local radius of curvature of the contour of the water bell in the x, y plane;
Q, total volume flux of water.

p is defined as positive if the pressure outside the water bell is higher than the pressure inside. In this work it will be assumed that the dynamic pressure of the surrounding air can be neglected and p is accordingly an imposed constant static pressure difference.

It turns out to be convenient to use a natural co-ordinate system (e.g. see Taylor 1959*a*) as shown in figure 1. The unit vectors $\mathbf{e}_s$ and $\mathbf{e}_\theta$ define the local tangent plane and the unit vector $\mathbf{e}_n$ is in the direction of the normal. The angle ϕ is defined as the angle between $\mathbf{e}_x$ and $\mathbf{e}_s$. The velocity field is given by

$$\mathbf{v} = u\mathbf{e}_s + v\mathbf{e}_\theta \tag{2.1}$$

and the values of u and v at $(0, y_0)$ are u_0 and v_0. If the thickness of the water sheet is assumed to be very small, implying that the velocity is locally approximately constant across the sheet, the balance of momentum in the $\mathbf{e}_n$ direction reads

$$\frac{2\Gamma}{\lambda} + \frac{2\Gamma\cos\phi}{y} - p + \rho g h\sin\phi - \frac{\rho h u^2}{\lambda} - \frac{\rho h v^2\cos\phi}{y} = 0. \tag{2.2}$$

The first two terms represent the contributions from the surface tension. The third and fourth terms give the effects of the pressure difference and the gravitational acceleration. The fifth and sixth terms are the centrifugal accelerations due to the velocities in the $\mathbf{e}_s$ and $\mathbf{e}_\theta$ directions respectively. Apart from the last term, (2.2) has been given by, among others, Taylor (1959*a*). If the motion of the ambient air is neglected, the only force affecting the energy of the water particles is the gravitational force and the energy equation becomes

$$u^2 + v^2 - 2gx = u_0^2 + v_0^2. \tag{2.3}$$

Under the same assumption, the angular momentum of the water particles is conserved, which implies that

$$v = y_0 v_0 / y. \tag{2.4}$$

Following Taylor (1959*a*), a characteristic length scale R is defined as

$$R = \rho Q u_0 / 4\pi\Gamma. \tag{2.5}$$

Using R as the length scale in the problem means that the force balance is mainly governed by inertia and surface tension. In what follows, the following non-dimensional length variables will be used:

$$X = x/R, \quad Y = y/R, \quad S = s/R, \tag{2.6a–c}$$

where s is the dimensional arc length of the contour of the water bell in the x, y plane. Non-dimensional velocity components are defined as

$$U = u/u_0, \quad V = v/v_0. \tag{2.7a, b}$$

Using (2.3)–(2.7), one can, after some algebra, write (2.2) in the following non-dimensional form:

$$\left(\frac{U}{Y} - 1\right)\frac{d\phi}{dS} + \frac{\cos\phi}{Y} - \kappa + \frac{\delta\sin\phi}{UY} - \frac{\gamma^2 Y_0^2\cos\phi}{UY^4} = 0, \tag{2.8}$$

where

$$U = [1 + 2\delta X + \gamma^2(1 - Y_0^2/Y^2)]^{\frac{1}{2}} \tag{2.9}$$

is the non-dimensional velocity in the $\mathbf{e}_s$ direction and

$$\delta = \frac{Rg}{u_0^2}, \quad \kappa = \frac{2\pi R^2 p}{\rho Q u_0}, \quad \gamma = \frac{v_0}{u_0}, \quad Y_0 = \frac{y_0}{R}. \tag{2.10a–d}$$

Equation (2.8) was first derived by Kristiansson (1975). The non-dimensional parameters δ and κ, which were first used by Taylor (1959*a*) in a somewhat different form, measure the relative importance of the gravitational acceleration and the pressure difference compared with inertia. The parameter γ, defined by (2.10*c*), measures the relative importance of the rotation. In order to calculate the shape of the swirling water bell, (2.8) has to be supplemented with the geometrical relation

$$dX/dY = \cot\phi. \tag{2.11}$$

Equations (2.8) and (2.11) are to be solved subject to the initial condition

$$\phi = \phi_0 \quad \text{for} \quad X = 0, \quad Y = Y_0. \tag{2.12}$$

In the general case, (2.8) and (2.11) were found to be too complicated to be solved analytically. For $\delta = \kappa = 0$ or $\delta = \gamma = 0$, one can show that (2.8) and (2.11) can be solved in terms of elliptic integrals with rather complicated arguments. However, as no significant physical insight appears to emerge from such solutions, (2.8) and (2.11) was solved numerically by using a standard library computer program for a system of coupled nonlinear ordinary differential equations of first order. Some interesting physical aspects of the problem, though, can be obtained by perturbing the exact solution given by Taylor (1959*a*) for $\delta = \kappa = \gamma = 0$ for small values of γ. Such a solution is given in the next section.

It should once again be pointed out that neglecting the motion of the ambient air may be an unacceptable approximation for rapidly moving and thin water sheets. This effect was first noted by Taylor (1959*a*) and has been calculated by Wegener & Parlange (1964) and Parlange (1967). The latter authors showed that the toroidal vortical motion set up by the air enclosed by the water bell may produce a dynamic pressure which, if these vortex motions are sufficiently strong and the inertia of the water sheet is sufficiently weak, may lead to a significant distortion of the shape of the water bell. The air outside the bell appears to have a minor effect. Parlange (1967) gave a successful approximate method of correcting for the dynamic pressure of the enclosed air. Although the method given by Parlange can probably be generalized to swirling water bells, this is outside the scope of the present work.

3. Perturbation solution for small γ, $\delta = \kappa = 0$

For $\delta = \kappa = 0$, one can write (2.8) in the following form:

$$\frac{\sin\phi}{\cos\phi}d\phi = \left[\frac{\alpha^2\beta}{Y(Y^2-\alpha^2)(\beta(Y^2-\alpha^2)^{\frac{1}{2}}-Y^2)} - \frac{Y}{\beta(Y^2-\alpha^2)^{\frac{1}{2}}-Y}\right]dY, \tag{3.1}$$

where the parameters α and β are defined by

$$\beta = (1+\gamma^2)^{\frac{1}{2}}, \quad \alpha = \gamma Y_0/\beta. \tag{3.2a, b}$$

Equation (3.1) can be integrated once, giving

$$\cos\phi = \vartheta Y/[\beta(Y^2-\alpha^2)^{\frac{1}{2}} - Y^2], \tag{3.3}$$

where ϑ is defined by

$$\vartheta = \cos\phi_0(1-Y_0). \tag{3.4}$$

It is readily verified that for $\gamma = 0$ equation (3.3) reduces to the corresponding equation given by Taylor (1959*a*). The singular cases $\cos\phi_0 = 0$ or $Y_0 = 1$ correspond,

in the case $\gamma = 0$, to a flat sheet of water (Taylor 1959*a*) and are not dealt with in this work. The admissible values of Y_0 deserve some comment. Taylor (1959*b*) demonstrated experimentally and theoretically, from a somewhat heuristic mathematical model, that a non-swirling water bell cannot exist in a region where the local Weber number W, which in the present notation is defined as

$$W = Y/U, \tag{3.5}$$

is greater than one. It is shown in the appendix that this condition holds approximately in the rotating case as well for reasonable parameter values. In the non-swirling case, the condition $W < 1$ is equivalent to $Y < 1$ according to (2.9) and it is consequently assumed in this section that $Y_0 < 1$.

In the following, a small parameter ϵ defined by $\epsilon = \gamma$ will be used. It is also assumed that $Y_0 = O(1)$. This restriction can be relaxed at the cost of some extra algebra. However, it turns out that no important physical properties of the solution are lost if this assumption is made.

Some information about the behaviour of the solution of (3.3) and (2.11) can be obtained by calculating the values of Y for which $\cos\phi = 1$, i.e. the radii where the radial motion of the water particles reverses. Expanding α and β, defined by (3.2*a*, *b*), in powers of ϵ, one finds from (3.3) the equation

$$Y^2(Y+\vartheta)^2 = Y^2 + \epsilon^2(Y^3 - Y_0^2) + O(\epsilon^4), \tag{3.6}$$

which has the following approximate positive solutions:

$$Y = 1 - \vartheta + \tfrac{1}{2}\epsilon^2[1 - Y_0^2/(1-\vartheta)^2] + O(\epsilon^4) \tag{3.7}$$

and

$$Y = \epsilon Y_0/(1-\vartheta^2)^{\frac{1}{2}} + O(\epsilon^2). \tag{3.8}$$

The second-order correction term in (3.7) is always positive for $Y_0 < 1$. Thus, for realistic boundary conditions, the maximum radius is slightly displaced outwards as could have been expected on physical grounds. The root (3.8) is rather interesting because it means that the water bell never reaches the axis of rotation, as it does in the non-swirling case. This can easily be explained in physical terms. A water particle moving inwards will spin up owing to the conservation of angular momentum [see (2.4)]. At a distance of order ϵ from the axis of rotation, the swirl velocity will be of order unity. This means that the water particle will experience an additional centrifugal force of order unity, which will move the particle outwards. Some further conclusions can be drawn by examining the structure of (2.11) and (3.3). First, dX/dY is a function of Y only, which reflects the fact that the motion is reversible in the $\mathbf{e}_x$ direction if $\delta = 0$. Second, for each value of Y, there are two values of dY/dX with the same absolute value but different signs. The presence of the two points where the radial velocity reverses thus means that the contour of the water bell will be periodic along the axis of rotation.† Moreover, the upper half of the contour between two turning points at the same radial distance will be the mirror image of the lower half. This property prevails, as will be discussed in the next section, also for finite values of γ and non-zero values of κ. In practice, however, the length of a swirling water bell will be limited by Kelvin–Helmholtz instability phenomena.

† The authors owe this argument to Professor B. J. Andersson.

In order to calculate a perturbation solution of (3.3) and (2.11), the two regions $Y = O(1)$ and $Y = O(\epsilon)$ have to be considered separately, because, as was discussed above, the physical processes are different in the two regions. For $Y = O(1)$, the zeroth-order solution is the one given by Taylor (1959*a*):

$$X^o = \vartheta\left[\operatorname{arccosh}\left(\frac{1}{\cos\phi_0}\right) - \operatorname{arccosh}\left(\frac{1-Y}{\vartheta}\right)\right]$$

$$\text{for} \quad 0 \leqslant X^o \leqslant \vartheta \operatorname{arccosh}\left(\frac{1}{\cos\phi_0}\right), \quad Y_0 \leqslant Y \leqslant 1-\vartheta; \tag{3.9a}$$

$$X^o = \vartheta\left[\operatorname{arccosh}\left(\frac{1}{\cos\phi_0}\right) + \operatorname{arccosh}\left(\frac{1-Y}{\vartheta}\right)\right]$$

$$\text{for} \quad \vartheta \operatorname{arccosh}\left(\frac{1}{\cos\phi_0}\right) \leqslant X^o < X_N - O(\epsilon), \quad O(\epsilon) < Y \leqslant 1-\vartheta. \tag{3.9b}$$

Where it has been assumed that $\phi_0 > 0$, X_N is defined by

$$X_N = \vartheta \operatorname{arccosh}\left[\frac{1+(1-\vartheta^2)^{\frac{1}{2}}\sin\phi_0}{\vartheta\cos\phi_0}\right] \tag{3.10}$$

and the superscript o denotes the 'outer' solution. For $Y = O(\epsilon)$, it is convenient to use a stretched co-ordinate ζ defined by

$$\zeta = Y/\epsilon \tag{3.11}$$

and to represent X, to lowest order, by

$$X = \epsilon X^i + X_N, \tag{3.12}$$

where the superscript i denotes the 'inner' solution. From (3.3), (2.11), (3.11) and (3.12) one finds, after some algebra, that

$$\frac{dX^i}{d\zeta} = -\frac{\vartheta}{(1-\vartheta^2)^{\frac{1}{2}}}\frac{\zeta}{[\zeta^2 - Y_0^2/(1-\vartheta^2)]^{\frac{1}{2}}}, \tag{3.13}$$

which can be integrated to

$$X^i = -\frac{\vartheta}{(1-\vartheta^2)^{\frac{1}{2}}}\left(\zeta^2 - \frac{Y_0^2}{1-\vartheta^2}\right)^{\frac{1}{2}} + X_0^i, \tag{3.14}$$

where X_0^i is a constant. By matching (3.14) and (3.9*b*), one finds that X_0^i is zero. A uniformly valid expansion can be written as

$$X = \vartheta\left[\operatorname{arccosh}\left(\frac{1}{\cos\phi_0}\right) + \operatorname{arccosh}\left(\frac{1-Y}{\vartheta}\right)\right] + \frac{\vartheta}{(1-\vartheta^2)^{\frac{1}{2}}}\left\{Y - \epsilon\left[\left(\frac{Y}{\epsilon}\right)^2 - \frac{Y_0^2}{1-\vartheta^2}\right]^{\frac{1}{2}}\right\}$$

$$\text{for} \quad \vartheta \operatorname{arccosh}\left(\frac{1}{\cos\phi_0}\right) \leqslant X \leqslant X_N, \quad \frac{\epsilon Y_0}{(1-\vartheta^2)^{\frac{1}{2}}} \leqslant Y \leqslant 1-\vartheta. \tag{3.15}$$

The solutions (3.9*a*) and (3.15) describe the part of the periodic solution between the initial value Y_0 and the point where the radial velocity first reverses near the axis of rotation. It should be noted that the periodic extension of (3.9*a*) and (3.15) is not uniformly valid for a large number of periods. For the parameter values $Y_0 = 0{\cdot}8$, $\phi_0 = \frac{1}{4}\pi$ and $\epsilon = 0{\cdot}20$, figure 2 shows a comparison between part of the periodic ex-

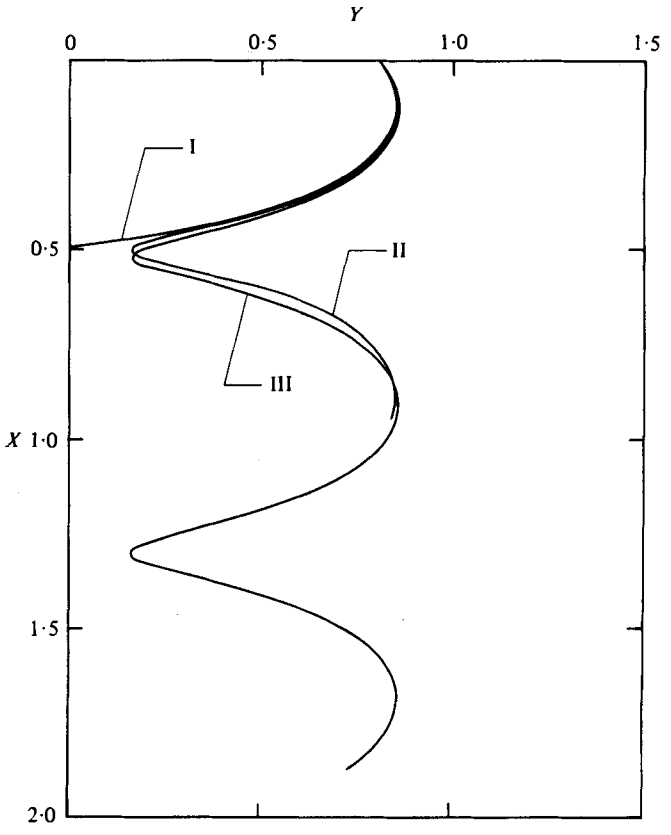

FIGURE 2. I, Taylor's (1959*a*) solution; II, perturbation solution; III, numerical solution.

tension of (3.9*a*) and (3.15) and a numerical solution of (2.8) and (2.11) with an estimated error less than $0{\cdot}5 \times 10^{-3}$. The solution given by Taylor (1959*a*) for $\epsilon = 0$ is also shown in figure 2.

It would be desirable to have the next-order correction to the perturbation solution (3.15). However, it turns out that the next-order correction to the outer solution is singular at $Y = 1-\vartheta$ and that the same kind of singularity appears for the next-order correction for the inner solution at $Y = \epsilon Y_0/(1-\vartheta^2)^{\frac{1}{2}}$. It can be shown that these singularities can be removed by introducing two additional boundary layers of thickness ϵ^2. Unfortunately, the algebra required for calculating these layers and matching the solutions in the four different regions is quite involved, therefore the calculation of the first-order correction to (3.15) was not attempted.

4. Some general properties of swirling water bells

Some illuminating results can be obtained by calculating the values of Y where the radial velocity reverses. This was done for $\delta = \kappa = 0$ and small values of γ in the previous section. For the same values of δ and κ but arbitrary values of γ, these values of Y are given by the positive roots of the equation

$$Y^4 + 2\vartheta Y^3 + (\vartheta^2 - 1 - \gamma^2)\, Y^2 + \gamma^2 Y_0^2 = 0, \tag{4.1}$$

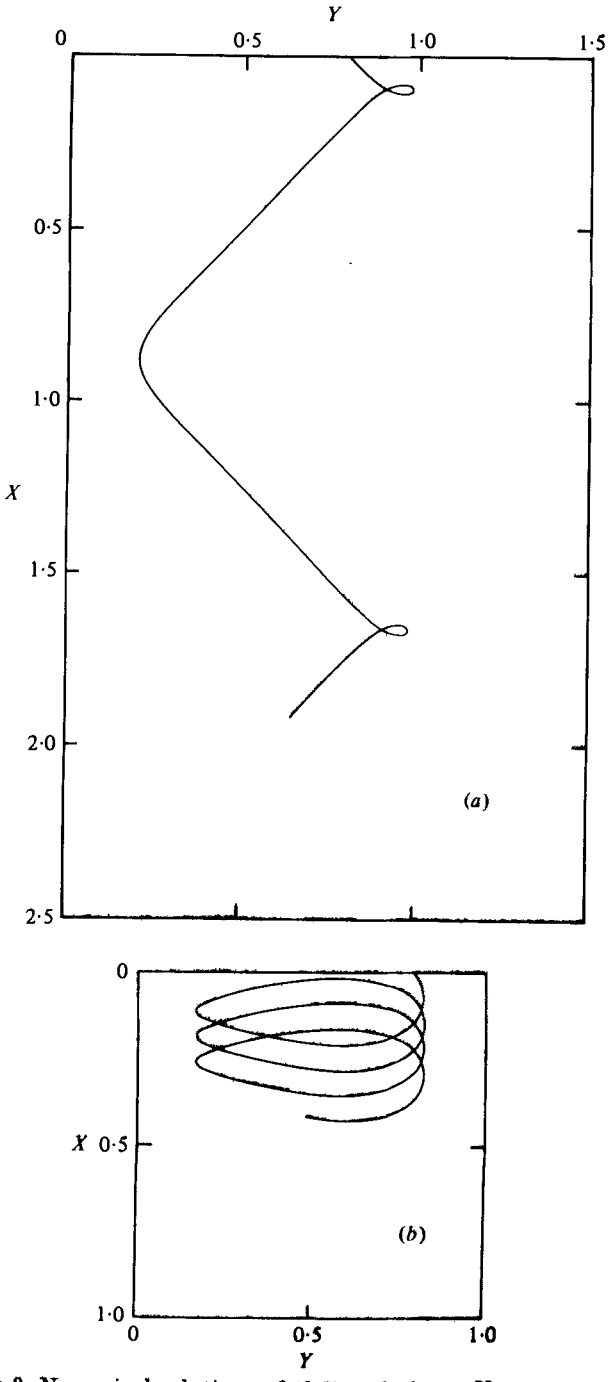

FIGURE 3. Numerical solutions of (2.8) and (2.11). $Y_0 = 0{\cdot}8$, $\phi_0 = \frac{1}{4}\pi$, $\gamma = 0{\cdot}2$, $\delta = 0$. (*a*) $\kappa = -1$. (*b*) $\kappa = +1$.

where ϑ is defined by (3.4). Equation (4.1) follows from (3.3) after inserting $\phi = 0$ and using the definitions (3.2*a*, *b*) of α and β. Although the roots of (4.1) can be calculated exactly, the resulting expressions are rather complicated so only a qualitative discussion will be carried out. The discussion will also be restricted to the case $\cos\phi_0 = 1$, i.e. $\vartheta = 1 - Y_0$. This means that one root ($Y = Y_0$) of (4.1) is given. From (2.9) and (3.5) one finds that the necessary condition $W < 1$ for the existence of a swirling water bell can (see the appendix) be written as

$$Y^4 - (1+\gamma^2)\, Y^2 + \gamma^2 Y_0^2 < 0. \tag{4.2}$$

From (4.2) it follows that one must require that $Y_0 < 1$. It is readily shown that the condition $Y_0 < 1$ implies that there are two positive roots, or one positive double root, of (4.1) and that these roots are enclosed by the roots of the equation $W = 1$ for all values of γ. This means that the class of water bells considered will never break up owing to violation of the condition (4.2) and will thus be infinitely long. It is also readily shown that if

$$\gamma^2 > Y_0 \tag{4.3}$$

the water bell will move radially outwards from $Y = Y_0$, $X = 0$, whereas a motion towards the axis of rotation will occur if $\gamma^2 < Y_0$. These results quantify the obvious fact that a sufficiently strong rotation will fling the water bell outwards. In the limit $\gamma^2 \to Y_0$, the water bell degenerates to a straight circular cylinder.

It should be noted that a swirling water bell need not be confined to the region $Y < 1$, as is the case for a non-swirling water bell. For instance, for large values of γ one finds that the second root of (4.1) is given approximately by

$$Y = \gamma - \vartheta + O(\gamma^{-1}). \tag{4.4}$$

It was shown by Lance & Perry (1953), who solved (2.8) and (2.11) numerically for $\gamma = 0$, that the contour of a non-swirling water bell may have cusps if $\kappa \neq 0$. In their numerical solutions bifurcation points appear and the computed curves have closed loops. Because a moving sheet of water cannot pass through itself, it was concluded that the contour of the physical water bell would have a cusp. Lance & Perry (1953) also made experiments, the results of which were in reasonable agreement with the theoretical predictions. As expected, cusps of this kind appear also for swirling water bells. Figures 3(*a*) and (*b*) show two numerical solutions of (2.8) and (2.11) for $\delta = 0$ but non-zero values of κ. The values of γ, ϕ_0 and Y_0 are the same as for the numerical solution shown in figure 2. The periodic properties of the solutions prevail also for non-zero values of κ, as can be expected on physical grounds.

5. Experimental procedure

Swirling water bells were produced by using the apparatus shown in figure 4. The apparatus was made of brass. Parts A, B and C are rotating and parts D and E are fixed. Part B is a turbowheel which is driven pneumatically by an air jet which, in turn, is driven by a small compressor. Part F is an axial seal. The water flow is shown by thick dark arrows. In the upper part of part A, there are twelve vertical channels with square cross-sections. Between the lower parts of parts A and C, there is a narrow annular slit. The apparatus works as follows. Non-rotating water enters

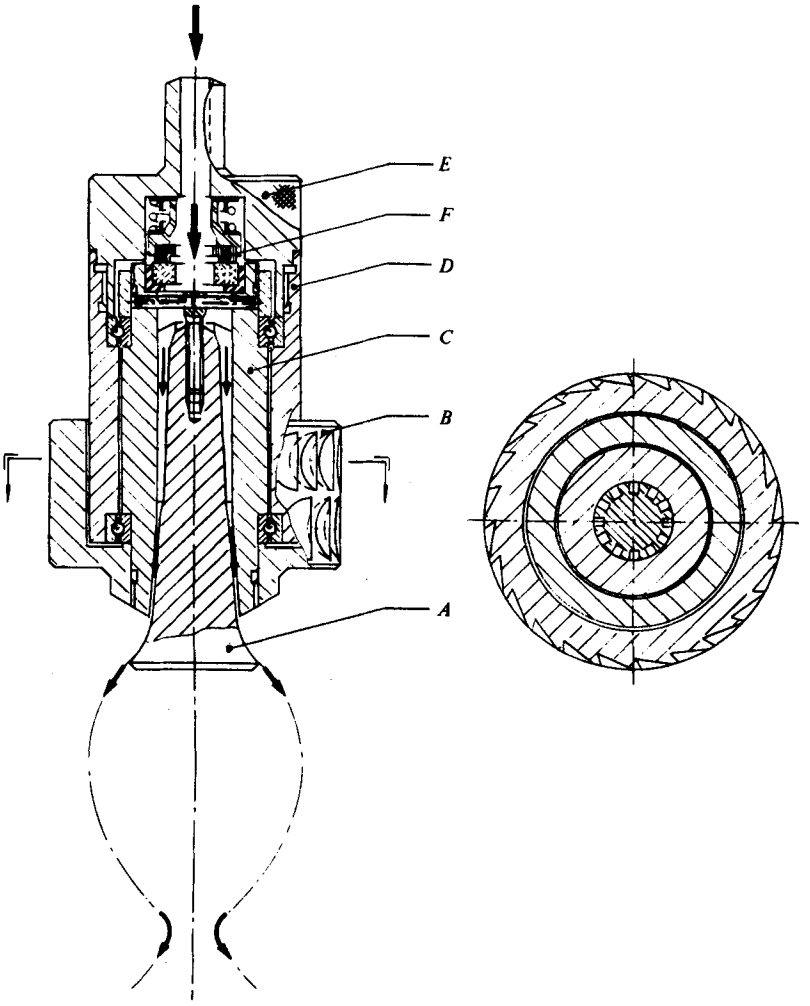

FIGURE 4. Sketch of apparatus used to produce swirling water bells.

from above into the cavity in the non-rotating part *E*. The water then enters the rotating vertical channels in part *A* and is thereby spun up. Thereafter the rotating water enters the narrow annular slit between the lower parts of parts *A* and *C*, comes out of this slit and flows on the lower part of part *A* and finally leaves part *A* at a sharp edge. In this way the swirl velocity of the water sheet can be controlled rather well. Part *A* can be displaced vertically relative to part *C*, whereby the width of the annular slit can be varied from 0·2 to 0·5 mm. The diameter of part *A* at the sharp edge is 32 mm and the distance from the axis of symmetry to the slit is 10 mm. By shielding the turbowheel from the water bell, it was found that the air jet which drives the turbowheel did not affect the shape of the water bell. The rotation rate was measured with an optical Ono Sokki HT-430 tachometer. The volume flux was measured with a Floscan 300-1 fluxmeter.

In order to investigate the flow leaving the channels in part *A* and entering the cavity between the parts *A* and *C*, an apparatus was made of Plexiglas with identical

	Volume flux Q (m³/s)	Width of slit (m)	R (m)	u_0 (m/s)	γ	δ	κ	Y_0	ϕ_0
Figure 5(*a*)	$2{\cdot}8\times10^{-5}$	3×10^{-4}	$7{\cdot}7\times10^{-2}$	2·6	0·64	0·12	0·0	0·21	$\frac{1}{4}\pi$
Figure 5(*b*)	$2{\cdot}8\times10^{-5}$	4×10^{-4}	$6{\cdot}1\times10^{-2}$	2·0	0·65	0·15	0·0	0·26	$\frac{1}{4}\pi$
Figure 5(*c*)	$1{\cdot}9\times10^{-5}$	3×10^{-4}	$3{\cdot}4\times10^{-2}$	1·7	0·16	1·1	0·0	0·48	$\frac{1}{4}\pi$

TABLE 1

parts A and C. The water was partially marked with dye and the flow was observed visually in the light from a stroboscope, which was tuned to the rotation frequency. A very regular axial flow was observed, which showed that the water film was spun up in a well-controlled manner. The width of the slit between parts A and B could not be adjusted very accurately with the Plexiglas apparatus and in the experiments to be described the brass apparatus was used.

When using the previously described apparatus, there will, unfortunately, be a small but non-negligible momentum loss due to viscous effects on the motion of the sheet before it leaves the sharp edge. This means that if one calculates u_0 and v_0 at the sharp edge by using the mean axial and swirl velocities in the slit and assumes that the flow is inviscid, cf. (2.4) and (2.3), an error will be introduced. The viscous momentum loss will obviously be significantly smaller for the swirling motion than for the meridional motion. The meridional momentum loss could be corrected for by measuring the thickness of the sheet at some suitable position, as was done by optical methods by Göring (1959) and Dombrowski *et al.* (1960). Such measurements were, however, not made in the present investigation. The order of magnitude of the meridional momentum loss can be estimated by comparing the shape of a non-swirling water bell from an experiment with the shape obtained by solving (2.8) and (2.11) numerically for $\gamma = \kappa = 0$ and using the previous estimate for u_0 in the definitions of R and δ. It was found that the calculated water bell was typically 15–25% larger than the experimental one. As expected, the error was found to decrease if the Reynolds number based on the mean velocity in the slit and the width of the slit increased. If u_0 was adjusted to make the length (or diameter) of the calculated water bell agree with the experimental value, the theoretical and experimental shapes agreed to within less than 5%. The remaining deviation is presumably due to the dynamic pressure of the enclosed air. In the experiments made by Göring (1959), this effect is very important as was shown by Parlange (1967), who calculated the shape of the water bells in Göring's experiments very accurately by using a simplified model for the motion of the enclosed air. By comparing the parameter ranges in the present experiments and those made by Göring (1959), one finds that the effect of the moving enclosed air on the shape of the water bell should indeed be of the order of a few per cent.

6. Experimental results

Photographs from three experiments are shown in figures 5(*a*), (*b*) and *c* (plate 1). The parameter values for the experiments are given in table 1. The viscous momentum loss, which was discussed in the previous section, has been neglected when calculating

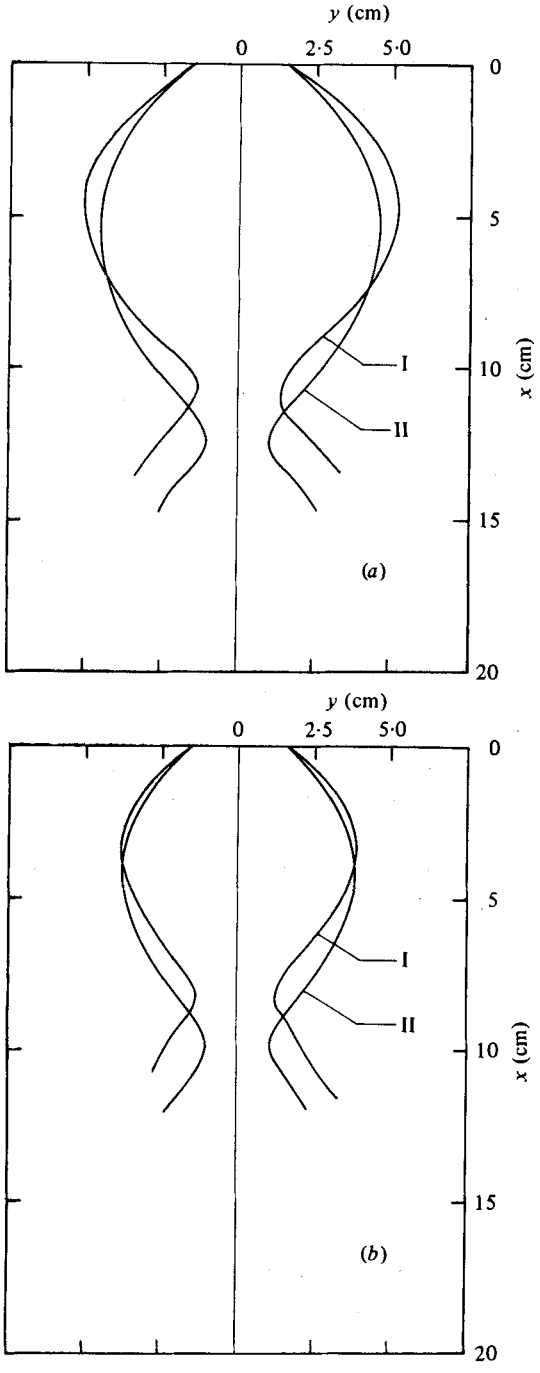

FIGURE 6. I, (*a*) shape of the bell in figure 5(*a*) and (*b*) shape of the bell in figure 5(*b*); II, numerical solution of (2.8) and (2.11) for the parameter values in table 1.

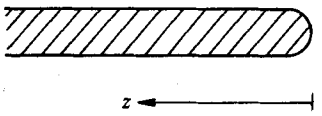

FIGURE 7. Definition of co-ordinate for describing the motion of a free edge.

these parameter values. The photographs show that the lengths of the water bells are obviously limited by a Kelvin–Helmholtz instability, which causes the bells in figures 5(*a*) and (*b*) to break up after approximately one-quarter of the second period and the bell in figure 5(*c*) after approximately one-quarter of the third period. It should be noted that the velocity of the water sheet in figure 5(*c*) is slower than that of the sheets in figures 5(*a*) and (*b*). This makes the bell in figure 5(c) more stable. The lower part of the bell is, however, strongly distorted by wave motions. Apart from such local wave motions and some very weak global oscillations, which were obviously caused by the rotating parts of the apparatus, the bells were in all cases steady and did last as long as desired. No systematic measurements of breakup lengths were made.

The shapes of the water bells in figures 5(*a*) and (*b*) are compared with numerical solutions of (2.8) and (2.11), for the parameter values given in table 1 in figures 6(*a*) and (*b*). The agreement between theory and experiment is reasonable. For reasons that will be discussed in a moment, the shape of the bell in figure 5(*c*) could not be predicted very well. The calculated bells shown in figures 6(*a*) and (*b*) are somewhat longer than the experimental ones. This is a consequence of the momentum loss caused by the contact of the water sheet with the solid surface, which has not been accounted for in the numerical solution. This error, which is relatively large for the water bell in figure 5(*c*), will give a reference velocity u_0 at the sharp edge which is too large in the numerical solution. The reference length R, defined by (2.5), will thus also be too large, giving a larger length scale for the calculated water bell than for the experimental one. However, the experimental and theoretical maximum diameters in figure 6(*b*) are roughly the same and in figure 6(*a*) the experimental maximum diameter is larger than the theoretical one, which would contradict the conclusion that R is too large. This can be explained by the fact that, because the value of u_0 used in the calculations is too large, the value of γ will be too small as the viscous effects on the swirl velocity are certainly significantly smaller than those on the meridional velocity. Too small a value of γ gives, of course, a decreased maximum diameter.

Professor Bengt Joel Andersson made it possible, by generously providing resources in his laboratory, to carry out the experimental part of this investigation. We are very grateful for this support. We are also indebted to him for many clarifying and stimulating discussions on the subject.

Appendix

Taylor (1959*b*) derived a condition for a free edge of a moving sheet of water to remain stationary in space by calculating how rapidly the surface tension will pull the free edge backwards. If the radial convection velocity of the sheet is in the opposite direction and has the same magnitude as the velocity of the edge caused by the

action of the surface tension, the edge will, according to Taylor (1959*b*), remain stationary in space. The model is somewhat crude as it does not account for the fact that water drops are shed periodically from the edge. However, the model describes the experiments made by Taylor (1959*b*) very well and it appears that the suggested physical process indeed determines the location of a free edge.

For a rotating sheet, Taylor's (1959*b*) mathematical model can be modified as follows. If the distance from the axis of rotation to the edge is large compared with the thickness of the sheet and it is assumed that the displacement of the edge is of the same order of magnitude as the thickness of the sheet, one can assume that the swirl velocity is approximately constant in the neighbourhood of the edge. The only dynamical effect of the swirl velocity near the edge will then be an approximately constant centrifugal force. Using the notation of § 2, one has the following dimensional equation of motion for a rotating free edge without any radial velocity (see figure 6*b*):

$$\frac{d}{dt}\left(m\frac{dz}{dt}\right) = 2\Gamma - \frac{mv^2}{y_e}, \tag{A 1}$$

where t is the time, m is the mass per unit length along the periphery of the sheet, v is the swirl velocity of the edge and y_e is the distance from the edge to the axis of rotation. The equation of continuity is

$$m = \rho h z, \tag{A 2}$$

where h is the thickness of the sheet near the edge and ρ is the density of the water. Following Taylor (1959*b*), it is assumed that the motion of the edge is such that h is approximately constant. From (A 1) and (A 2) one finds

$$z\frac{d^2z}{dt^2} + \left(\frac{dz}{dt}\right)^2 + Az = B, \tag{A 3}$$

where the positive constants A and B are defined by

$$A = v^2/y_e, \quad B = 2\Gamma/\rho h. \tag{A 4a, b}$$

The solution of (A 3) is given by (see Kamke 1959, p. 581)

$$t = \int_0^z \left(B - \frac{2Az}{3} + \frac{C}{z^2}\right)^{-\frac{1}{2}} dz, \tag{A 5}$$

where C is a constant of integration and the initial condition $z(0) = 0$ has been used. For dz/dt to be finite for $t = 0$, C has to be zero. One finds that

$$z = B^{\frac{1}{2}}t - \tfrac{1}{6}At^2. \tag{A 6}$$

Superimposing a radial velocity u, which can be done under the previously stated assumptions without significantly changing the dynamics, and introducing the non-dimensional length and time variables Z and T, defined by

$$z = Zh, \quad t = hT/u, \tag{A 7a, b}$$

one finds from (A 6), (A 4a, b) and (A 7a, b) that

$$z = (W^{\frac{1}{2}} - 1)\,T - \frac{\gamma^2 W^{\frac{1}{2}} R^{\frac{1}{2}} h}{6 y_e^{\frac{1}{2}}}\,T^2. \tag{A 8}$$

The local Weber number W in (A 8) is defined by

$$W = 2T/\rho h u^2 \tag{A 9}$$

and R is defined by (2.5). Usually h/y_e is very small and the remaining factors in the coefficient of T^2 in (A 8) are, under normal conditions, of order unity. This means that the last term in (A 8) will be important for large values of T only. However, the success of Taylor's (1959*b*) model indicates that the time scale for the periodic shedding of drops is h/u. The last term in (A 8) is therefore likely to remain small and the local criterion $W < 1$ for the existence of a water bell can be expected to hold approximately in the rotating case as well, at least for very thin sheets. It should be noted that the governing equations (2.8) and (2.11) as such may have solutions in regions where $W > 1$.

REFERENCES

Boussinesq, J. 1869 *C.R. Acad. Sci. Paris* **69**, 45, 128.

Boussinesq, J. 1913 *C.R. Acad. Sci. Paris* **157**, 89.

Dombrowski, N., Hasson, D. & Ward, D. E. 1960 *Chem. Engng Sci.* **12**, 35.

Göring, W. 1959 *Z. Elektrochem., Ber. Bunsenges. Phys. Chem.* **63**, 1069.

Kamke, E. 1959 *Differentialgleichungen*. Leipzig: Akademische Verlagsgesellschaft.

Kristiansson, L. P. 1975 *Swed. Roy. Inst. Tech. Dept. Mech. Tech. Rep.* no. 75–1.

Lance, G. N. & Perry, R. L. 1953 *Proc. Phys. Soc.* B **66**, 1067.

Parlange, J. Y. 1967 *J. Fluid Mech.* **29**, 361.

Savart, F. 1833 *Ann. Chem. Phys.* **54**, 55.

Savart, F. 1834 *Ann. Chem. Phys.* **55**, 257.

Stenström, L. 1971 *Alfa-Laval Tech. Rep.* TF 7102–03.

Taylor, G. I. 1959*a* *Proc. Roy. Soc.* A **253**, 289.

Taylor, G. I. 1959*b* *Proc. Roy. Soc.* A **253**, 313.

Wegener, P. P. & Parlange, J.-Y. 1964 *Z. Phys. Chem.* **43**, 245.

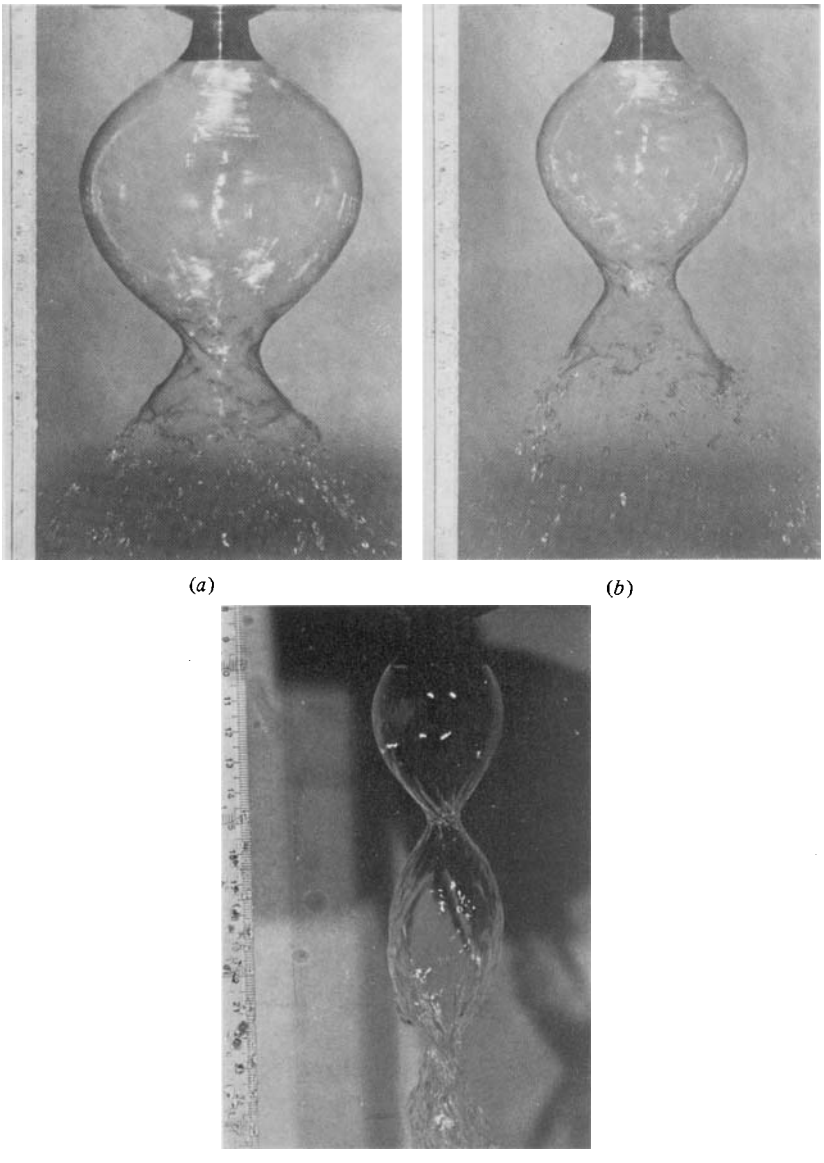

(*a*) (*b*)

(*c*)

FIGURE 5. Photographs of swirling water bells. The parameter values are given in table 1.